

## Coherent optical oscillator with periodic zero- $\pi$ phase modulation

Aleksandr Shumelyuk, Andrew Hryhorashchuk, and Serguey Odoulov\*

*Institute of Physics, National Academy of Sciences, 03650, Kiev-39, Prospekt Nauki 46, Ukraine*

(Received 21 May 2005; published 22 August 2005)

The four-wave-mixing coherent optical oscillator is described, which is emitting light wave with regular alternation of its phase between two discrete values zero and  $\pi$ . Such a periodic self-modulation is a consequence of competition of photorefractive gratings formed by movable charge species of two different signs. The period of modulation depends on overthreshold coupling strength and on decay time of slow photorefractive grating. It falls to few seconds range for  $\text{Sn}_2\text{P}_2\text{S}_6$  crystals at ambient temperature but it can go down to microsecond range for photorefractive semiconductors.

DOI: [10.1103/PhysRevA.72.023819](https://doi.org/10.1103/PhysRevA.72.023819)

PACS number(s): 42.65.Pc, 42.65.Sf, 42.65.Hw

### I. INTRODUCTION

Four-wave-mixing coherent optical oscillators generate optical waves with the wave vectors, wave fronts and polarization that can be different from that of the pump waves but with the temporal frequency which is either identical or very close to the pump frequency (see, e.g., [1]). While the spatial content of the oscillation beams and generation of the phase conjugate replicas of the incident pump beam [2,3] were investigated in detail and still are in the focus of many studies the temporal behavior of oscillation attracted much less attention of the researches. The only exception is an extensively studied topic of transition to chaotic behavior [4–7].

Usually with the cw pump wave(s) the oscillation intensity is either time independent, too, or features sinusoidal modulation thus revealing the excitation of two modes in the spectrum [8,9], or becomes irregular and chaotic for multimode (multigrating) oscillation [4–7]. We report in this paper on *observation of a new temporal behavior of coherent oscillator* with photorefractive  $\text{Sn}_2\text{P}_2\text{S}_6$ , which shows regular switches of the phase of oscillation wave between zero and  $\pi$  accompanied with synchronous modulation of output intensity. In this respect the oscillator under consideration resembles multivibrator (relaxation oscillator), an electronic circuit that consists of two cross-coupled transistors and continuously switches from one discrete state to the other [10].

The origin of the unusual operation regime in photorefractive  $\text{Sn}_2\text{P}_2\text{S}_6$  nests in simultaneous development of space charge gratings with considerably different decay times by two species of movable charge carriers with different signs [11]. With no external field applied to the sample the gratings recorded by carriers of different sign are complimentary, i.e., a grating recorded by redistribution of electrons is  $\pi$  shifted with respect to a grating recorded by holes. Therefore, a presence of two types of movable charge carriers results in inhibition of overall photorefractive grating and reduction of its diffraction efficiency and gain factor. The particularity of the reported operation mode of the coherent oscillator is caused by inherent possibility to develop not only two out-

of-phase photorefractive gratings but also two in-phase gratings, at least during a certain time in each oscillation pulse. Such an option exists in coherent oscillators with open cavities because the phase of the oscillation wave is predetermined neither by the resonance conditions for cavity modes nor by the phase of any external seed.

After disappearance of coherent oscillation at the end of every pulse the remaining part of long living (“slow”) photorefractive grating diffracts the pump wave in direction of cavity axis and produce in such a manner a rather strong seed for development of the in-phase fast grating in an oscillation pulse that follow. Quite quickly the overall space charge saturates at the level that is a sum of amplitudes of the fast grating and slow grating. Now a new slow grating starts to develop tending to compensate for the developed charge redistribution. This process lasts until the amplitude of overall space charge field drops down to the threshold value. The oscillation disappears, fast grating quickly decays to zero and the remaining part of the slow grating gives rise to development of the next oscillation pulse,  $\pi$  shifted in phase with respect to the previous.

In this paper the basic experimental observations are described, the model is presented, the additional experiments that justify the model are analyzed and finally some estimates are given.

### II. EXPERIMENT

The semilinear coherent oscillator with two counterpropagating pump waves 1 and 2 is studied (Fig. 1). The  $\text{Sn}_2\text{P}_2\text{S}_6$  (tin hypophosphite) crystal measuring  $9 \times 9 \times 4.5 \text{ mm}^3$  along  $X$ ,  $Y$ , and  $Z$  crystallographic directions is grown, poled, and optically finished at the Institute of Solid State Physics and Chemistry, Uzhgorod State University, Ukraine. The sample belongs to type 1  $\text{Sn}_2\text{P}_2\text{S}_6$  crystals [12] with the pronounced contribution of charge carriers of two signs in formation of the space charge grating. According to our estimates the lifetime of the fast grating formed by photoexcited holes is about 40 ms at the intensity about  $3 \text{ W/cm}^2$  and grating spacing  $2 \text{ }\mu\text{m}$ , typical for our experiment, while the lifetime of the “slow” grating formed by the thermally excited electrons is about 12 s.

The TEM<sub>00</sub> output of He-Ne laser with several longitudinal modes is used as a pump radiation (50 mW power, about

\*Electronic address: [odoulov@iop.kiev.ua](mailto:odoulov@iop.kiev.ua); URL: <http://www.iop.kiev.ua/~prc>

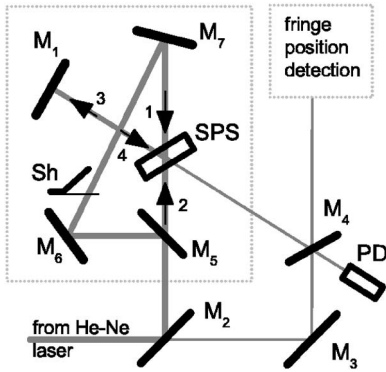


FIG. 1. The experimental setup.  $M$  are the mirrors; PD is a photodiode, Sh is a shutter, and  $\text{Sn}_2\text{P}_2\text{S}_6$  is a photorefractive sample.

1.4 mm Gaussian beam diameter in unexpanded beam). The mirror  $M_2$  reflects the main part of the laser intensity to form two counterpropagating pump waves 1 and 2 with the help of mirrors  $M_5$ ,  $M_6$ , and  $M_7$ . The shutter Sh is placed between the mirrors  $M_6$  and  $M_7$ , it is used to study the decay of the photorefractive grating when only one of the two pump waves is incident to the sample. The intensity ratio of two pump waves can be controlled with the help of neutral density filters put in front of the sample (not shown in the figure). A part of laser beam is sent with the help of the mirror  $M_3$  to the screen as a reference beam. Together with the oscillation beam directed to the screen with the help of the mirror  $M_4$  it forms fringes that allow to detect changes in the phase of the oscillation wave.

The pump waves enter [001] polished faces of the sample at an angle  $9^\circ$  (i.e.,  $81^\circ$  to  $x$  axis) is in plane of drawing of Fig. 1. A highly reflecting mirror of  $M_1$  closes the semilinear cavity. The mirrors are placed in a way to ensure mutual coherence of the pump wave 1 and oscillation wave 4 inside the sample. To fulfil this requirement the distance from mirror  $M_5$ - $M_6$ - $M_7$ -sample is chosen to be equal to the distance  $M_5$ -sample-sample- $M_1$ - $M_1$ -sample. The optical axis of the cavity formed by the sample and mirror  $M_1$  makes angle  $9^\circ$  with the normal to the sample face so that total angle between pump and oscillation waves is  $18^\circ$  in the air.

Both pump beams, as also oscillation beam are polarized in the plane of drawing thus optimizing the coupling between the pump and oscillation wave (the largest electrooptic coefficient  $r_{111} = 170$  pm/V [13] defines the amplitude of the refractive index grating). The experimental setup allows also measuring the dynamics of the oscillation intensity with photodiode PD.

With this configuration the coherent oscillation between the ordinary mirror  $M_1$  and phase conjugate mirror in photorefractive crystal has been achieved and studied. A typical temporal dynamics of oscillation is shown in Fig. 2(a). In every pulse the oscillation develops very rapidly and then starts to decrease gradually with the abrupt disappearance near the end of the pulse. The observation of the fringe pattern proved that it is immobile during whole pulse but moves abruptly to a half of fringe spacing when new pulse develops [Fig. 2(b)]. The fringe contrast varies according to the changes in oscillation intensity; the switching occurs every

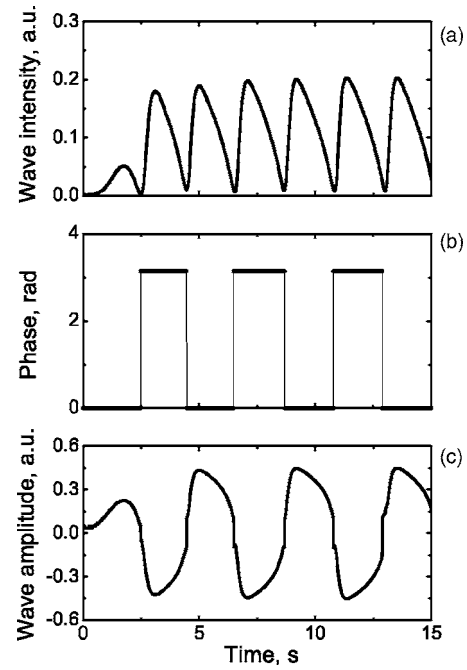


FIG. 2. Temporal variation of (a) oscillation wave intensity, (b) phase, and (c) amplitude.

time when oscillation intensity and fringe contrast passes through zero value. With the known temporal behavior of intensity and phase it is possible to reconstruct the electric field of the oscillation wave as it is shown in Fig. 2(c).

For several reasons (pronounced dark conductivity, intensity dependent effective trap density) the amplitude of a space charge grating in  $\text{Sn}_2\text{P}_2\text{S}_6$  depends on intensity. Thus the oscillation appears only above certain threshold of the pump wave intensity what is rather unusual for photorefractive oscillators. The peak value of oscillation intensity increases with pump as it is shown in Fig. 3(a) and the pulse duration increases with pump, too [Fig. 3(b)].

As it might be expected, the oscillation intensity is also sensitive to the pump beam intensity ratio [Fig. 4(a)] featur-

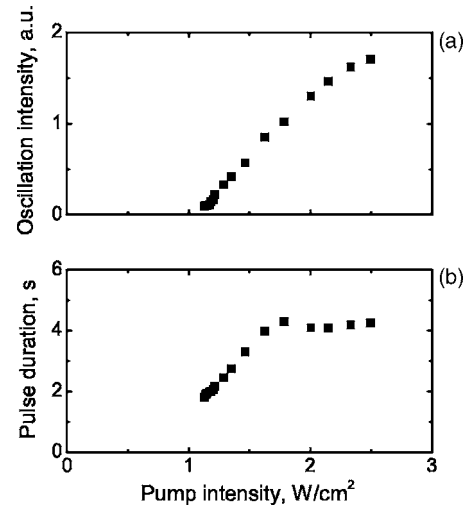


FIG. 3. Pump intensity dependence of (a) oscillation intensity and (b) pulse duration.

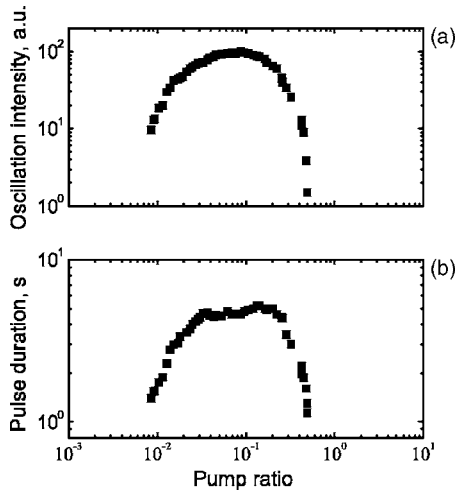


FIG. 4. Pump ratio dependence of (a) oscillation intensity and (b) pulse duration.

ing well defined threshold values where oscillation intensity vanishes to zero and beyond which it does not exist. The pump ratio dependence of the pulse duration is similar to that for oscillation intensity [Fig. 4(b)].

### III. MODEL

In this section we describe a qualitative model of the observed phenomenon, which is based on two specific assumptions: Only one type of movable charge carriers is photoexcited (holes) while the motion of other type of carriers (electrons) is thermally activated, and the formation of pulses in oscillation intensity is related mainly to changes of slow grating amplitude, the switching of the fast grating on and off is considered to be quasi instantaneous. Both these assumptions are well justified for  $\text{Sn}_2\text{P}_2\text{S}_6$  [11].

When virgin sample is exposed to two pump waves the coherent oscillation selfdevelops first because of formation of only one “fast” space charge grating [10] by photoexcited holes [14]. Before the beginning of oscillation no “slow” grating exists as movable electrons are generated thermally and not via photoexcitations [11]. When the oscillation wave appears the amplitude of the fast grating of photoexcited holes is growing from zero until it reaches its steady state. Now the thermally excited electrons start to redistribute in the created space charge field giving rise to secondary (“slow”) grating which is out of phase with respect to the initial one. The intensity of the oscillation wave is consequently decreasing [Fig. 2(a)]. For a certain amplitude of “slow” grating the overall gain becomes insufficient to support the oscillation and the system appears below the threshold. The amplitude of the fast grating decays and at a certain moment becomes equal to the amplitude of the slow grating. Both gratings compensate each other exactly and the intensity of the diffracted wave vanishes to zero.

Further on the amplitude of the fast grating is continuously decreasing becoming smaller than the amplitude of persisting slow grating. The phase of the emerging difference grating is now imposed by the phase of the slow grating, i.e.,

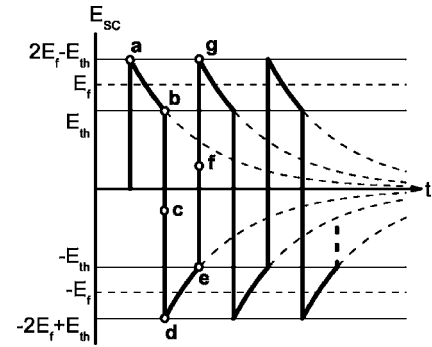


FIG. 5. Temporal variation of the space charge field.

is shifted to  $\pi$  with respect to the initially recorded grating. The smaller becomes the decaying fast grating the larger is the  $\pi$ -shifted difference grating. The diffraction from this grating serves now as a very strong seed for development of a new oscillation in a semilinear cavity. From this seed a new fast grating grows up which is in phase with the seeding slow grating. A new fast increase of the oscillation intensity occurs and the second spike in oscillation intensity appears. When fast grating reaches its saturation level for the second time the thermally excited electrons start to build the out-of-phase grating. This new grating at first compensates completely the slow seeding grating and then is still increasing in amplitude until the system appears below the threshold for the second time. Then this sequence is repeated in time leading to formation of consecutive pulses.

Altogether four contributions to the space charge grating with the same grating vector  $\mathbf{K}$  manifest themselves during one full pulsation period consisting of two consecutive pulses: Two out-of-phase “fast” gratings, one and the same during each half period, and two out of phase “slow” gratings. Their common effect is presented in Fig. 5 that shows temporal variation of the resulting space charge field amplitude  $E_{sc}$ . The positive and negative parts in this figure can be considered as the amplitudes of two complimentary space charge field gratings,  $E_{sc1} \cos(Kx)$  and  $E_{sc2} \cos(Kx + \pi) = -E_{sc1} \cos(Kx)$ . The horizontal lines  $\pm E_f$  and  $\pm E_{th}$  mark the saturated space charge field of the fast grating and space charge field of the oscillation threshold, respectively. Negative signs of  $E_f$  and  $E_{th}$  indicate that they are associated with the  $\pi$ -shifted grating  $sc2$ .

Let us start from the largest value of  $E_{sc}$  for already well developed pulsations, shown in Fig. 5 as a point  $a$ . Here both gratings, new fast and remaining from the previous pulse slow, are in phase and ensure largest possible oscillation intensity. With the progressing time  $E_{sc}$  decreases  $\propto \exp(-t/\tau_s)$  because of the build-up of a new slow grating (complete decay curves are shown by dashes in Fig. 5). This decrease ends up, however, at a point  $b$ , where total space charge field drops to the threshold value  $E_{th}$ . At this moment the oscillation disappears; thus the fast grating starts to decay, too, and the space charge field comes to a point  $c$  where  $E_{sc} = E_{th} - E_f$ . This happens with characteristic time  $\tau_f$  of a few milliseconds, i.e., instantaneously in a scale of Fig. 5.

For a complimentary grating  $E_{sc2} \cos(Kx + \pi) = -E_{sc1} \cos(Kx)$  the point  $c$  is a starting point for development

of a new fast grating, also with amplitude  $|E_f|$ . The overall space charge  $E_{sc}$  jumps to point  $d$ , where, once more, new fast and remaining slow gratings are in phase. After that a similar decay of  $E_{sc2}$  occurs: Slow decay to the threshold point  $e$  followed by fast decay to the point  $f$  and finally recording of a new fast grating with the end point  $g$ , what closes the cycle. At the point  $g$  the system returns to the state equivalent to that at the starting point  $a$ .

Thus the slow grating, when gradually growing in amplitude, inhibits overall gain for oscillation mode but at the same time it accumulates large seed for the other oscillation mode with  $\pi$ -shifted space charge grating. Here the analogy to electronic multivibrator becomes evident: every time when one of two coupled transistors of multivibrator is open it increases losses for itself and, at the same time, brings the amplifier on the second transistors closer to be open [10]. This supports the definition “optical multivibrator” given to the reported oscillation mode of photorefractive oscillator.

#### IV. JUSTIFYING EXPERIMENTS

To confirm the validity of the proposed model we study the decay of the space charge grating at different characteristic positions within a separate pulse. To observe the decay curves the pump wave 1 is stopped with a shutter Sh (see Fig. 1) at a certain moments within the pulse. The detector PD measures in this case temporal variation of the diffraction efficiency of the decaying grating.

We expect that near the peak of the oscillation intensity the two space charge gratings are perfectly in phase. This should give a decay curve which is biexponential with no singularities throughout total time of measurements. At the end of the oscillation pulse, when its intensity is approaching to zero, the two space charge gratings are expected to be present as well, but this time with the  $\pi$  shift between them. This suggests the appearance of a deep in the decay curve, which corresponds to the moment of complete compensation of two gratings when their amplitudes becomes identical. Finally, for the intermediate oscillation intensity, roughly two times smaller than the peak value, the amplitude of the slow component should be strongly reduced as compared to two previous decay curves.

Figure 6 shows three measured decay curves that illustrate the above cases, for largest (a), intermediate (b), and smallest (c) oscillation intensity.

In Fig. 6(a) one can see smooth decay with continuous change of the slope what proves that both gratings, slow and fast, are in phase. In Fig. 6(b) only one, fast grating manifests itself: after decay of fast grating the measured intensity drops to the noise level what can be seen from much smaller intensity as also from larger spread of the measured values. In Fig. 6(c) once more the decay curve consists of two pronounced parts with different slopes close to that in Fig. 6(a). The distinction is that just at the moment when the “weights” of two gratings, fast and slow, became equal the diffracted intensity drops to zero. This proves unambiguously that two contributions are out of phase in this case. In such a way the results of this experiment confirm the predictions of our model.

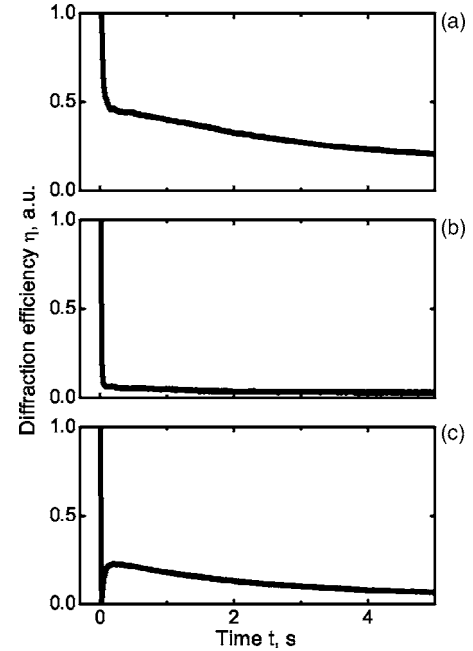


FIG. 6. Decay of the grating efficiency when pump wave is abruptly stopped at the maximum of oscillation pulse (a), at the intermediate intensity (b), and at the smallest oscillation intensity at the end of the pulse (c).

One more qualitative prove of the model validity relates to particularity of the first pulse in repetitive rate regime shown in Fig. 2(a). According to the model the first pulse develops from the scattering seed only, there is no slow grating remaining from the previous pulse for the very first pulse of oscillation. Thus the overthreshold space charge field for the beginning of the first pulse is  $E_f - E_{th}$ , while for any pulse for well established oscillations it is twice as large,  $2(E_f - E_{th})$ . This difference in overthreshold values must result in weaker first pulse compared to following pulses, its amplitude should be at least two times smaller. This prediction agrees well with the experimental observations, as shown in Fig. 2(a).

#### V. ESTIMATES FOR GRATING AMPLITUDES

From the experimental data presented above one can extract parameters of the  $\text{Sn}_2\text{P}_2\text{S}_6$  sample and considered coherent oscillator. The oscillation condition reads

$$RR_{PC} = 1, \quad (1)$$

i.e., the losses that are due to incomplete reflectivity  $R$  of the conventional mirror (all other oscillation losses can be included in effective  $R$ , too) should be compensated for by amplified reflection of phase conjugate mirror  $R_{PC}$ . The phase conjugate reflectivity of the sample is [15]

$$R_{PC} = \frac{\sinh^2(\Gamma\ell/4)}{\cosh^2(\Gamma\ell/4 - (\ln r)/2)} \quad (2)$$

for frequency degenerate oscillation.

The most informative is the pump ratio dependence of the oscillation intensity [Fig. 4(a)]. As it follows from Eq. (2) the

largest phase conjugate reflectivity (and therefore largest output intensity) correspond to  $(\Gamma\ell/2)=\ln r$ . This allows estimating the coupling strength that is ensured by  $\text{Sn}_2\text{P}_2\text{S}_6$  sample:  $\Gamma\ell \approx 5.4$ .

The other way to evaluate  $\Gamma\ell$  give the values of  $r$  where oscillation disappears, the threshold values,  $r_1=0.08$  and  $r_2=0.5$  [Fig. 4(a)]. The oscillation threshold corresponds to one and the same value of  $R_{PC}$  that is equal to  $1/R$ . This allows to write that  $\ln r_1 - (\Gamma\ell/2) = (\Gamma\ell/2) - \ln r_2$  and to get  $\Gamma\ell = 5.5$ . In addition, Eq. (2) provides a value for an effective reflectivity of conventional mirror that incorporates all kinds of cavity losses:  $R=0.78$ . With this data we can find now the threshold value of the coupling strength  $(\Gamma\ell)_{th}=4.1$ , for pump ratio  $r=0.07$  that is optimized for the best output.

The above estimates are related to the fast component in grating recording because just fast component is responsible for the oscillation switch-on at the threshold. The estimates for slow component can be done from the known pulse length in coherent oscillation. Neglecting the difference in the screening and diffusion lengths for movable charge carriers we can write for dynamics of slow grating [16]

$$(\Gamma\ell)_s = (\Gamma\ell)_f^{max} [1 - \exp(-t/\tau_s)] \approx (\Gamma\ell)_f^{max} t/\tau_s. \quad (3)$$

Taking the running time  $t$  equal to the pulse length  $\Delta t$  we get  $(\Gamma\ell)_s^{max} = (\Gamma\ell)_f^{max} (\Delta t/\tau_s)$ . With  $\Delta t=5$  s,  $(\Gamma\ell)_f=5.4$  and  $\tau_s=12$  s the slow grating can develop up to  $(\Gamma\ell)_s=1.8$ . It should be underlined that this estimated value is not the ultimate amplitude for  $(\Gamma\ell)_s^{max}$  [which is equal to  $(\Gamma\ell)_f^{max}$  within the assumptions made] but a value reached in this particular experiment for this particular set of parameters  $R, r, (\Gamma\ell)_f^{max}$ .

## VI. TEMPORAL VARIATION OF THE GAIN SPECTRUM

The reported periodic pulsations reveal the interaction which is by definition non-degenerate in frequency. The Fourier spectrum of function shown in Fig. 2(c) consists of multiple frequency harmonics what fits well to definition of optical multivibrator [10]. Let us underline once more that this operation mode is qualitatively different and can not be reduced to the known sinusoidal modulation of the oscillation intensity, with only two symmetric oscillation frequencies in the spectrum [16].

To explain nondegenerate steady state coherent oscillation in different photorefractive oscillators it is useful to consider the dependence of two-beam coupling gain (or phase conjugate reflectivity  $R_{pc}$ ) on frequency detuning  $\Omega$  of the oscillation wave with respect to the pump waves, i.e., gain spectrum. Figure 7 shows the gain spectrum at saturation [Fig. 7(a)] and temporal transformations of the gain spectrum for optical multivibrator [Fig. 7(b)].

With cw pump waves and in assumption of very small transport lengths [17] the gain spectrum has a deep with zero value exactly at degenerate frequency [Fig. 7(a)]:

$$\Gamma\ell(\Omega) = \frac{(\Gamma\ell)_f^{max}}{1 + (\tau_f\Omega)^2} - \frac{(\Gamma\ell)_s^{max}}{1 + (\tau_s\Omega)^2}. \quad (4)$$

The cw oscillation was expected to appear at two frequencies shifted symmetrically with respect to the pump fre-

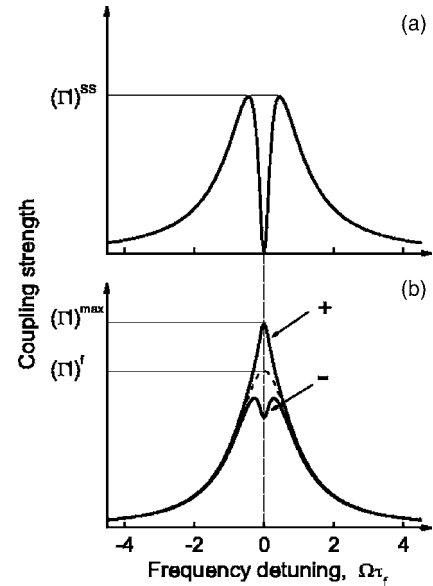


FIG. 7. (a) Typical dependence of the steady-state gain factor on frequency detuning in crystals with strong electron-hole competition. (b) Three snapshots of the gain spectrum for particular oscillation pulse of optical multivibrator: “+” corresponds to in-phase slow and fast gratings while “-” for out-of-phase gratings; solid line shows time average spectrum.  $\Gamma\ell^{max}$ ,  $\Gamma\ell^{ss}$ , and  $\Gamma\ell^f$  show, respectively, maximum coupling strength for multivibrator, maximum steady state coupling strength for cw mode of operation, and maximum coupling strength for only one fast grating.

quency, that ensure the largest steady-state gain factor,  $\Gamma\ell^{ss}$ . This prediction was confirmed experimentally for coherent oscillator with ring-loop cavity described in [16]. For the considered semilinear coherent oscillator one could expect the same behavior, i.e., the excitation of steady state oscillation with two different frequencies at the maxima of gain spectrum. Thus a question arises why pulsed mode of oscillation (multivibrator) appears to be preferable.

While we do not have at present the exact answer to this question we can guess that the reason lies in larger gain that is ensured in multivibrator mode of operation as compared to steady state cw operation. This can be explained with the help of Fig. 7(b) in which the snapshots of gain spectrum are shown for the beginning of the oscillation pulse (curve marked as “+”) and at the end of the pulse (curve marked as “-”). It is obvious that maximum gain for curve “+” is much larger than maximum steady state gain in curve of Fig. 7(a), because it is given by equation similar to Eq. (4) but with the sum and not difference of two terms in the right-hand side. Thus at least at the beginning of pulse the gain for oscillation wave in multivibrator mode of operation is larger than in regular cw regime. It is important to add also that the gain factor at  $\Omega=0$ ,  $\Gamma\ell^f$  average over the pulse duration is larger than the maximum gain factor in Fig. 7(a), too. This might be a reason why we observe just a multivibrator mode of operation in semilinear coherent oscillator and not a regular cw frequency degenerate operation like in [17].

The temporal spectrum of multivibrator consists, as it was mentioned already, of multiple frequencies and the frequency separation between components is quite different from that

known for two-frequency oscillation described in [16]. Usually it is smaller than in two-frequency operation mode [16]. Moreover, the dependences of frequency shifts  $\Delta\Omega$  on over-threshold coupling strength  $E_f - E_{th}$  are qualitatively different:  $\Delta\Omega$  is increasing for multivibrator while it is going down to zero at the threshold of two-frequency oscillation [17].

## VII. CONCLUSIONS

A new repetition rate mode of operation of a coherent photorefractive oscillator is described, with high precision switches of the phase of oscillation wave between zero and  $\pi$  in consecutive pulses. A model is proposed, based on competition of the space charge gratings that are created in the sample with movable charge carriers of opposite sign. This

model explains qualitatively well the experimental results; it is confirmed also by justifying experiments.

It should be noted that the observed oscillation mode can occur not only in  $\text{Sn}_2\text{P}_2\text{S}_6$  crystals but in any material with two competing gratings possessing quite different decay times. According to our estimates a suitable potential candidate may be photorefractive CdTe with pronounced electron-hole competition in space charge grating formation (see, e.g., Ref. [18]). Taking into account much smaller decay time for photorefractive semiconductors it might be expected that the characteristic frequency of pulsations will go to kHz range and even higher.

## ACKNOWLEDGMENTS

We are grateful to Dr. A. Grabar and Dr. I. Stoyka for  $\text{Sn}_2\text{P}_2\text{S}_6$  sample.

- 
- [1] S. Odoulov, M. Soskin, and A. Khyzhnjak, *Coherent Oscillators with Four Wave Mixing (Dynamic Grating Lasers)* (Harwood Academic Publishers, London, Chur, 1989).
  - [2] C. Denz, M. Schwab, M. Sedlatschek, T. Tschudi, and T. Honda, *J. Opt. Soc. Am. B* **15**, 2057 (1998).
  - [3] B. Ya Zel'Dovich, A. V. Mamaev, and V. V. Shkunov, *Speckle-Wave Interactions in Application to Holography and Nonlinear Optics* (CRC Press, Boca Raton, 1995).
  - [4] *Measures of Complexity and Chaos*, edited by N. V. Abraham, A. M. Albano, A. Passamante, and P. E. Rapp (Plenum, New York, 1989).
  - [5] F. T. Arecchi, G. Giacomelli, P. L. Ramazza, and S. Residori, *Phys. Rev. Lett.* **65**, 2531 (1990).
  - [6] D. J. Gauthier, P. Narum, and R. W. Boyd, *Phys. Rev. Lett.* **58**, 1640 (1987).
  - [7] Siuying R. Liu and G. Indebetouw, *J. Opt. Soc. Am. B* **9**, 1507 (1992).
  - [8] S. G. Odoulov, A. N. Shumelyuk, G. Brost, and K. Magde, *Appl. Phys. Lett.* **69**, 3665 (1996).
  - [9] P. Mathey, S. Odoulov, and D. Rytz, *Phys. Rev. Lett.* **89**, 053901 (2002).
  - [10] H. Abraham and E. Bloch, *Ann. Phys. (Paris)* **12**, 237 (1919); see also <http://en.wikipedia.org/wiki/Multivibrator>
  - [11] S. Odoulov, A. Shumelyuk, U. Hellwig, R. Rupp, A. Grabar, and I. Stoika, *J. Opt. Soc. Am. B* **13**, 2352 (1996).
  - [12] A. Shumelyuk, S. Odoulov, D. Kip, and E. Kraetzig, *Appl. Phys. B: Lasers Opt.* **72**, 707 (2001).
  - [13] D. Haertle, G. Caimi, A. Haldi, G. Montemezzani, A. A. Grabar, I. M. Stoika, and Yu. M. Vysochanskii, *Opt. Commun.* **215**, 333 (2003).
  - [14] I. Seres, S. Stepanov, S. Mansurova, and A. Grabar, *J. Opt. Soc. Am. B* **17**, 1986 (2000).
  - [15] L. Solymar, D. J. Webb, and A. Grunnet-Jepsen, *The Physics and Applications of Photorefractive Materials* (Clarendon Press, Oxford, 1996).
  - [16] A. Shumelyuk, S. Odoulov, and G. Brost, *Appl. Phys. B: Lasers Opt.* **68**, 959 (1999).
  - [17] A. Shumelyuk, S. Odoulov, and G. Brost, *J. Opt. Soc. Am. B* **15**, 2125 (1998).
  - [18] A. Shumelyuk, K. Shcherbin, S. Odoulov, B. Sturman, E. Podivilov, and K. Buse, *Phys. Rev. Lett.* **93**, 243604 (2004).